Strongly Correlated Growth of Rydberg Aggregates in a Vapor Cell

A. Urvoy, F. Ripka, I. Lesanovsky, D. Booth, J. P. Shaffer, T. Pfau, and R. Löw

Phys. Rev. Lett. **114**, 203002 — Published 19 May 2015

DOI: 10.1103/PhysRevLett.114.203002

Strongly correlated growth of Rydberg aggregates in a vapor cell

A. Urvoy,[1,*] F. Ripka,[1] I. Lesanovsky,[2] D. Booth,[3] J.P. Shaffer,[3] T. Pfau,[1] and R. Löw[1,†]

[1] *5. Physikalisches Institut and Center for Integrated Quantum Science and Technology, Universität Stuttgart, Pfaffenwaldring 57, 70550 Stuttgart, Germany*

[2] *School of Physics and Astronomy, University of Nottingham, Nottingham, NG7 2RD, UK*

[3] *Homer L. Dodge Department of Physics and Astronomy, The University of Oklahoma, 440 West Brooks Street, Norman, Oklahoma 73019, USA*

(Dated: March 9, 2015)

The observation of strongly interacting many-body phenomena in atomic gases typically requires ultracold samples. Here we show that the strong interaction potentials between Rydberg atoms enable the observation of many-body effects in an atomic vapor, even at room temperature. We excite Rydberg atoms in cesium vapor and observe in real-time an out-of-equilibrium excitation dynamics that is consistent with an aggregation mechanism. The experimental observations show qualitative and quantitative agreement with a microscopic theoretical model. Numerical simulations reveal that the strongly correlated growth of the emerging aggregates is reminiscent of soft-matter type systems.

PACS numbers: 32.80.Ee, 34.20.Cf, 03.65.Yz, 61.43.Hv

Due to their exaggerated properties, Rydberg atoms find applications in various research fields ranging from cavity QED [1], quantum information [2], quantum optics [3–7], microwave sensing [8] to molecular physics [9]. One particular area of research employs the strong interactions between Rydberg atoms to create strongly interacting many-body quantum systems for quantum simulation [10–12], quantum phase transitions [13] and the realization of correlated or spatially ordered states [14–18]. In any system, gaseous, liquid, glass or solid, spatial correlations can only arise if interactions are present. In Rydberg gases these correlations have recently been revealed by the direct imaging of the resonant excitation blockade effect [17, 19]. In our experiment an initially nearly ideal gas of thermal atoms at room temperature is excited into a strongly interacting Rydberg state. The Rydberg excitations show correlated many-body dynamics that shares similarities with that of soft-matter systems.

We consider the situation of a dense atomic gas, where dense means that the mean inter-particle distance is smaller than the typical interaction distance. The interplay between these strong interactions and an off-resonant excitation laser results in a non-equilibrium dynamics with pronounced spatial correlations (related is the antiblockade in ultracold atoms [20, 21]). At a certain distance r_{fac} from a Rydberg atom the interaction shifts the Rydberg states in resonance with the detuned excitation light fields, as depicted in Fig. 1(a). The subsequent resonant excitations are restricted to specific distances and therefore result in the formation of so-called aggregates that feature non-trivial spatial correlations [22–25]. This so-called facilitated excitation occurs predominantly at the boundary of aggregates [see Fig. 1(b)], similarly to seeded nucleation. The number of Rydberg excitations grows increasingly faster as the size of the aggregates gets larger. After a certain time a (quasi) steady state is reached and the excitation saturates because the sample is maximally filled with Rydberg atoms. The spatial correlations expected for this steady state are depicted in Fig. 1(b). The density-density correlation function sketched here shows an enhanced probability for finding two atoms separated by the facilitation radius r_{fac}. There is no apparent long-range order since the isotropic facilitation mechanism does not favor the creation of crystalline arrangements. The existence of such Rydberg aggregates has recently been observed in ultracold systems [24, 25]. In these studies the Rydberg number distributions were extracted and matched to the results of empirical rate equation models, proving the existence of small aggregates with up to 8 excitations.

In this Letter we investigate a complementary regime and study the dynamics of the aggregation process in an atomic vapor at room temperature. Central parameters such as the dephasing rate and the atomic density are up to 2 orders of magnitude larger than in previous work [24, 25]. To quantify the non-equilibrium dynamics we perform a systematic study of the characteristic time scale that underlies the aggregation process. We find that the functional dependence of this time scale on various system parameters can be approximated by power laws. The corresponding exponents agree well with those obtained from a theoretical aggregation model. Further evidence for the aggregation dynamics is found through a quantitative evaluation of the number of Rydberg excitations and the resulting mean inter-particle distance which is consistent with the existence of a facilitation radius.

We perform our experiments in a gas of cesium atoms at room temperature or above. The cesium atoms are confined in a 220 μm thick glass cell [see Fig. 2(b)]. The atomic density N_{g} ranges from 10 $\mu\mathrm{m}^{-3}$ to 500 $\mu\mathrm{m}^{-3}$,

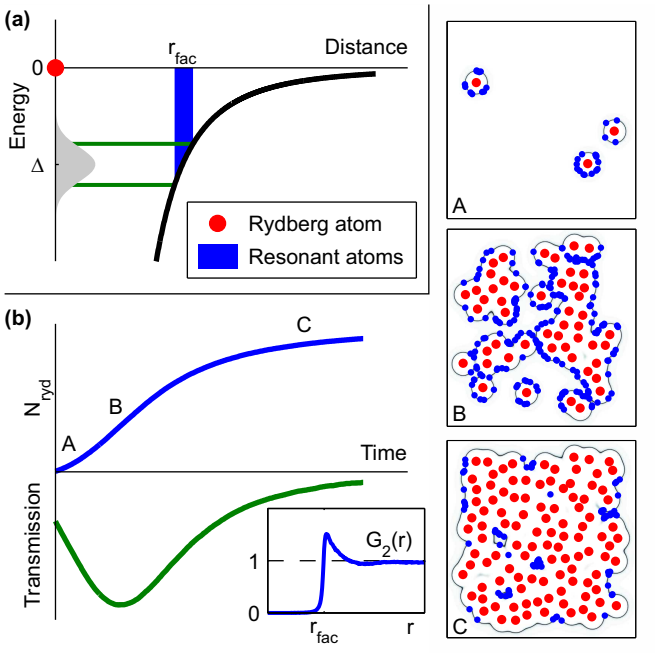

FIG. 1. Principle of the aggregation. (a) Interaction induced level shift. An already excited Rydberg atom (red dot) at the origin produces an energy shift for the neighboring atoms. At the facilitation radius $r_{\rm fac}$, the atoms are exactly shifted in resonance with the excitation laser, red-detuned by Δ. The grey shaded area symbolizes the excitation bandwidth, a Gaussian whose width is given by the dephasing rate γ. (b) Left: Typical time evolution of the Rydberg population and of the transmission change of the exciting laser [experimental signal, which is proportional to the derivative of the Rydberg density, see text and Fig. 2 for details] during the aggregation process. Right: Snapshots of the aggregation at times A, B and C, illustrated for a frozen gas in 2D. Red dots correspond to Rydberg atoms. Blue dots correspond to resonant atoms. The dark grey line shows the 'resonant shell' in which the excitation of Rydberg atoms is facilitated. Inset: Sketch of the density-density correlation function expected for the steady state [corresponding to (C)].

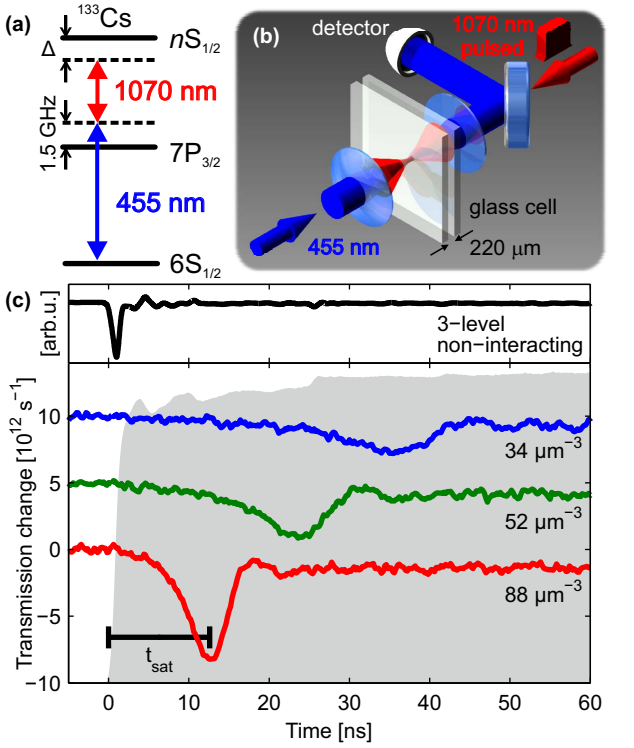

FIG. 2. (a) Schematic energy level diagram for the excitation to Rydberg states of cesium atoms. (b) Sketch of the experimental setup. (c) Transmission signals at different atom number densities for the 32S state. The two-photon detuning is $\Delta \approx 2\pi \times -2200$ MHz. The two-photon Rabi frequency is $\Omega = 2\pi \times 100$ MHz. The grey-shaded area in the background represents the temporal pulse shape of the infrared laser. The time delay $t_{\rm sat}$ used for the quantitative analysis is also depicted. The black curve (upper panel) is the expected transmission signal (not to scale) for non-interacting atoms (following the approach from Ref. [31]).

which is large compared to previous experiments on interacting Rydberg atoms in thermal vapor [26–28] and non-BEC cold atomic gases [24, 25, 29] where $N_{\rm g} \lesssim 10\ \mu{\rm m}^{-3}$. We excite cesium atoms from the ground state $6{\rm S}_{1/2}$ to a Rydberg state $n{\rm S}_{1/2}$ off-resonantly via the intermediate state $7{\rm P}_{3/2}$ [see Fig. 2(a)]. The two-photon transition is red-detuned by Δ with respect to the unperturbed Rydberg state. The lower transition is driven by a cw laser at 455 nm, which also serves as the probing field. For the upper transition a laser at $\sim$ 1070 nm is pulsed on the nanosecond scale using a fast Pockels cell. The effective Rabi frequency of the two-photon transition is then given by $\Omega = \Omega_{455}\,\Omega_{1070}/(2\,\delta_{7{\rm P}})$, where Ω_{455} and Ω_{1070} are the respective single transition Rabi frequencies and $\delta_{7{\rm P}} = 1.5$ GHz is the detuning to the intermediate state [30]. We measure the transmission change of the lower 455 nm laser after suddenly switching on the upper 1070 nm laser on. Note that this signal is directly proportional to the time derivative of the Rydberg population [30]. Typical transmission traces are shown in Fig. 2(c) for various atom number densities. Immediately after the 1070 nm laser is switched on (at t = 0) atoms are transferred to the Rydberg state, and for each excited Rydberg atom one photon is removed from the probe resulting in a decrease of the transmission.

One striking feature is the large red detuning of up to 10 GHz at which these signals are observed, in contrast to previous work on coherent excitation in a more dilute gas [27, 31]. Line broadenings and shifts to the blue have been observed with S-states in cold atoms [24], and Rydberg aggregates have been observed only at blue detunings [24, 25], as expected from the repulsive Rydberg-Rydberg interaction potential for most Rydberg S-states [32]. However at large atomic densities, the mean interparticle distance is so small that the perturbative character of the van-der-Waals potential is not valid anymore. Level crossings between pair states now have to

be considered. For Rydberg S-states in cesium a strong resonant dipole-quadrupole interaction with neighboring pair-states occurs at 0.55 μm for $n = 32$ [30, 33]. Initially dipole-forbidden attractive pair states acquire some nS-nS admixture at short inter-atomic distances due to the dipole-quadrupole interaction. Therefore the Rydberg-Rydberg interaction for S-states in cesium also features an effective attractive component, allowing for us to observe an excitation signal at large red detuning.

A first indication for the collective nature of the excitation dynamics is provided by the data in Fig. 2. Here we consider the characteristic time scale of the excitation $t_{\rm sat}$, i.e. the time at which the transmission reaches its minimum [as shown in Fig. 2(c)]. In the non-interacting case this time scale is given by $1/\Delta \sim 0.1$ ns (black line). In the experiment however the excitation signal is slow ($t_{\rm sat} \gg 1/\Delta$) and density dependent, which is only possible if many-body effects are included. Pulse propagation effects can be excluded due to the small optical depth at the large detunings applied.

To analyze the dynamics, we systematically varied all accessible parameters independently: Δ, Ω, $N_{\rm g}$ and n^*, where $n^* = n - \delta$ is the effective principal quantum number of the Rydberg state, δ being the quantum defect. Only the dephasing rate γ, determined by the Doppler shifts, the velocity of the atoms and the steep slope of the pair-state potentials, cannot easily be tuned over a significant range (for the derivation of the actual dephasing rate, see Supplemental Material [30]). The basic experimental settings are the following: $\Delta \approx 2\pi \times -2200$ MHz, $\Omega = 2\pi \times 100$ MHz, $N_{\rm g} = 36$ μm^{-3} and $n^* = 27.95$ (32S state), and are all but one kept constant. First, by fitting the values of the time scale of the excitation $t_{\rm sat}$ against Δ we obtain a power law as $t_{\rm sat} \propto |\Delta|^a$ with $a = 1.99(14)$. In the same way, we find that $t_{\rm sat} \propto \Omega^b$ with $b = -2.10(5)$. The power law for $N_{\rm g}$ is $t_{\rm sat} \propto N_{\rm g}^c$ with $c = -1.09(6)$. Finally we performed density scans at three different principal quantum numbers (32S, 34S and 36S states) and were able to extract a scaling behavior as $N_{\rm g}^{-1}(n^*)^d$ with $d = -4.6(5)$. These results are summarized in Table I.

By integrating the transmission signal over time we obtain an estimate of the actual number of Rydberg atoms present in the sample. At the time when the Rydberg excitation starts to saturate the Rydberg number in the excitation volume reaches approximately 50000 atoms. The corresponding mean inter-atomic distance is $\langle r \rangle = 0.65$ μm, leading to approximative values for the effective van-der-Waals or dipole-dipole strength of interaction as $C_\alpha = \Delta \times \langle r \rangle^\alpha$ [22] with $C_6 = 2\pi \times -109$ MHz $\cdot$ μm^6 and $C_3 = 2\pi \times -405$ MHz $\cdot$ μm^3 (at $\Delta \approx 2\pi \times -1500$ MHz). We use these values as an input for simulations described in the following.

We compared these findings to the results of the Rydberg aggregation model adapted from Ref. [22]. This model describes the dynamics of Rydberg aggregation within a system of two-level atoms in the presence of strong dephasing. This central assumption of strong dephasing applies to the experimental situation discussed here since the motion-induced dephasing is larger than the Rabi frequency ($\gamma \gtrsim 2\pi \times 0.5$ GHz [30]). The reduction to a two-level system is well justified in our case, although the commonly used adiabatic elimination of the intermediate state typically breaks down for quantitative considerations of the coherent evolution [27, 31]. Here however, because of the large dephasing rates due to the atomic motion we do not observe coherent evolution, and because of the large detunings we expect only less than 1.5% population of the intermediate state. We performed simulations for an ensemble of randomly distributed atoms in 3D, assuming a pure van-der-Waals ($V_{\rm vdW} = C_6/r^6$) or pure dipole-dipole ($V_{\rm dd} = C_3/r^3$) attractive interaction potential. In fact the actual experimental potential curves have a more complex spatial dependence, due to strong state mixing [30]. The latter makes the actual microscopic description of the excitation dynamics rather intricate since a two-level description of an atom might not be sufficient for covering all possible pair excitation channels. Therefore the van-der-Waals and dipole-dipole potential that are used in our two-level model should be regarded as the limiting approximations of the actual experimental situation. We evaluate the time scale of the excitation $t_{\rm sat}$ defined by the transmission minimum, as in the experiment. All results are listed in Table I. We find an excellent agreement between the experimental and theoretical exponents. In particular the dependence of $t_{\rm sat}$ on approximately Ω^{-2} indicates that a strong dephasing effect is present in our system [22]. Moreover the power laws vary only slightly,

	Δ[a]	Ω[b]	$N_{\rm g}$[c]	n^*[d]
Exp	1.99(14)	−2.10(5)	−1.09(6)	−4.6(5)
vdW	2.15(1)	−2	−0.86(1)	−4.72(5)
dd	2.38(0)	−2	−0.74(1)	−2.95(2)

[a] Range: -4.5 ... -1.3 GHz
[b] Range: 75 ... 175 MHz
[c] Range: 28 ... 101 μm^{-3}
[d] Range: 32S - 34S - 36S

TABLE I. Power laws for the aggregation delay $t_{\rm sat}$. In the experiment ('Exp'), the parameters are $\Delta \approx 2\pi \times -2200$ MHz, $\Omega = 2\pi \times 100$ MHz, $N_{\rm g} = 36$ μm^{-3} and $n = 32$, or varied over the specified range. The power laws labeled as 'vdW' and 'dd' were extracted from simulations in an ensemble of randomly and uniformly distributed atoms with van-der-Waals (ensemble of 10^3 atoms) dipole-dipole interaction (ensemble of 15^3 atoms) respectively, using the parameters from the experiment and the extracted interaction strengths (see text). The dephasing rate was also extracted from the experiment [30]. All uncertainties represent the confidence region of the fits. No uncertainty is given for the exponent of Ω in the theory, fixed at -2 as by the assumption of strong dephasing.

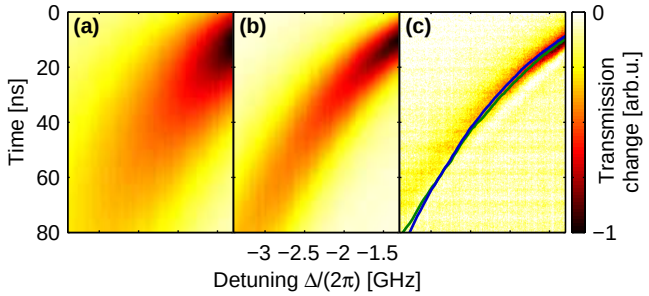

FIG. 3. Density plots showing the transmission change as a function of time (vertical axis, from top to bottom) and detuning. The parameters are as in Table I. (a) Simulated data with pure van-der-Waals interaction. The Rabi frequency was rescaled with a factor 0.38. (b) Simulated data with pure dipole-dipole interaction (for 15^3 atoms). The Rabi frequency was rescaled with a factor 0.23. (c) Experimental data. The blue (resp. green) line shows the position of the absorption maximum $t_{\rm sat}$ in the simulated data with van-der-Waals (resp. dipole-dipole) interaction.

independently of whether pure van-der-Waals or pure dipole-dipole interaction are used. Our experimental results are compatible with both potentials, suggesting a rather weak dependence on the actual shape of the potential and that the basic mechanism of aggregation only relies on the existence of a facilitation radius.

In Fig. 3(a) [resp. (b)] we show the transmission change extracted from the model with van-der-Waals [resp. dipole-dipole] interaction and in Fig. 3(c) from the experiment. The quantitative agreement for the time scale $t_{\rm sat}$ between theory and experiment is excellent. Due to the complex pair state potentials and strong state-mixing that are crucial here, an adaptation of the Rabi frequency has to be performed in order to use the two-level model (i.e. a model with a single Rydberg state). In our simulations the Rabi frequency is reduced by a factor of 0.38 (for van-der-Waals interaction) and 0.23 (for dipole-dipole interaction) compared to the experiment. These factors are compatible with the nS-nS admixture that one can extract from the pair-state potentials [30]. Note that with dipole-dipole interaction there is a dependence on the system size due to the long-range character of the $1/r^3$ potential, hence the different rescaling factors applied in Fig. 3(a) and 3(b).

The comparison of the experimental results to those of the model show that facilitated excitation is occurring, which implies that an aggregation dynamics takes place. The frozen gas approximation which is used to model the aggregation in [22] holds strictly for time intervals of about 0.3 ns, the transit time of the atoms through the 'resonant shell' (see Figure 1). During this time aggregates consisting of up to 4 atoms are formed [30]. Their spatial correlations will then quickly decay to those of a non-interacting ideal gas. Note, however, that even after that time the aggregation of excitations continues at the boundary of the uncorrelated aggregates.

Despite this effect the agreement between the experimental values of $t_{\rm sat}$ and those obtained from the simple theoretical model is in general good [see Fig. 3]. Yet the time evolution differs as the experimental signal appears much more narrow in time than in the simulations. We attribute this discrepancy to the inherent differences between the microscopics of the experimental system and the theoretical model (e.g. the complex potentials and the atomic motion). Interestingly, when considering the temporal width of the signal, the simulations with dipole-dipole interaction seem to agree best with the experiment, which is realistic considering that one component of the actual interaction potentials is of pure dipole-dipole nature. Moreover, the model does not account for the fact that the excitation of isolated, i.e. not facilitated, atoms is in fact coherent.

Another feature of the experimental data that is not reproduced by the theory is the small overshoot in transmission just before the system reaches the steady state [for instance at 20 ns for $N_{\rm g} = 88\ \mu{\rm m}^{-3}$ in Fig. 2(a)]. Remnants of coherent Rabi oscillations can be ruled out given the large dephasing rates and large detunings with respect to the single-atom resonance. Moreover the time scale of the overshoot, e.g. the time between the two maxima, does not show a specific dependency on the detuning, as is the case for Rabi flopping. Explaining this feature will require further study and a more sophisticated theory. Note that ion effects can be neglected. There are no ions in the sample prior to the excitation, otherwise they would act as aggregation seeds [35] at $t = 0$ and change the signal dramatically. Moreover plasma formation would occur only once Rydberg atoms have been excited [34] and therefore cannot explain our Rydberg excitation signal. In spite of the low collisional ionization rate (~ 40 MHz [34]) it might happen that in the course of the experiment single ions are created. However single ions will not disturb the aggregation dynamics, because of the similarity between the ion-Rydberg and the Rydberg-Rydberg potentials [35].

In conclusion, we have shown a facilitated excitation process of Rydberg atoms in thermal vapor. We have characterized the dynamics by measuring power laws for all relevant experimental parameters. These power laws, as well as absolute numbers for the dynamics and Rydberg density are in excellent agreement with those from a model for Rydberg aggregation. These results were obtained in the framework of thermal vapors, but the general ideas also apply to experiments in ultracold atoms. In the ultracold regime it would be interesting to study how quantum effects influence the aggregation time scale when the strength of dephasing noise is systematically lowered.

The authors would like to thank D. Peter, S. Weber, S. Hofferberth and J.P. Garrahan for fruitful discussions, as well as H. Kübler for proof reading. This project was

supported by the Carl-Zeiss-Stiftung and the ERC under contract number 267100. I.L. acknowledges funding from the European Research Council under the European Union's Seventh Framework Programme (FP/2007-2013) / ERC Grant Agreement n. 335266 (ESCQUMA) and the EU-FET Grant No. 512862 (HAIRS). D.B. and J.P.S. acknowledge financial support from grants NSF(PHY-1205392) and DARPA(60181-PH-DRP) for this work. We acknowledge the European Union H2020 FET Proactive project RySQ (grant N. 640378).

* Electronic address: a.urvoy@physik.uni-stuttgart.de
† Electronic address: r.loew@physik.uni-stuttgart.de

[1] S. Haroche, Rev. Mod. Phys. **85**, 1083 (2013).
[2] M. Saffman, T. G. Walker, and K. Mølmer, Rev. Mod. Phys. **82**, 2313 (2010).
[3] Y. O. Dudin and A. Kuzmich, Science **336**, 887 (2012).
[4] T. Peyronel, O. Firstenberg, Q.-Y. Liang, S. Hofferberth, A. V. Gorshkov, T. Pohl, M. D. Lukin, and V. Vuletić, Nature **488**, 57 (2012).
[5] D. Maxwell, D.J. Szwer, D. Paredes-Barato, H. Busche, J.D. Pritchard, A. Gauguet, K.J. Weatherill, M.P.A. Jones, and C.S. Adams, Phys. Rev. Lett. **110**, 103001 (2013).
[6] H. Gorniaczyk, C. Tresp, J. Schmidt, H. Fedder, and S. Hofferberth, Phys. Rev. Lett. **113**, 053601 (2014).
[7] D. Tiarks, S. Baur, K. Schneider, S. Dürr, and G. Rempe, Phys. Rev. Lett. **113**, 053602 (2014).
[8] J. A. Sedlacek, A. Schwettmann, H. Kübler, R. Löw, T. Pfau, and J. P. Shaffer, Nature Physics **8**, 819 (2012).
[9] V. Bendkowsky, B. Butscher, J. Nipper, J. P. Shaffer, R. Löw, and T. Pfau, Nature **458**, 1005 (2009).
[10] H. Weimer, M. Müller, I. Lesanovsky, P. Zoller, and H. P. Büchler, Nature Physics **6**, 382 (2010).
[11] G. Günter, H. Schempp, M. Robert-de Saint-Vincent, V. Gavryusev, S. Helmrich, C. S. Hofmann, S. Whitlock, and M. Weidemüller, Science **342**, 954 (2013).
[12] S. Ravets, H. Labuhn, D. Barredo, L. Béguin, T. Lahaye, and A. Browaeys, Nature Physics **10**, 914 (2014).
[13] R. Löw, H. Weimer, U. Krohn, R. Heidemann, V. Bendkowsky, B. Butscher, H.P. Büchler, and T. Pfau, Phys. Rev. A **80**, 033422 (2009).
[14] T. Pohl, E. Demler, and M. D. Lukin, Phys. Rev. Lett. **104**, 043002 (2010).
[15] F. Cinti, P. Jain, M. Boninsegni, A. Micheli, P. Zoller, and G. Pupillo, Phys. Rev. Lett. **105**, 135301 (2010).
[16] R. M. W. van Bijnen, S. Smit, K. A. H. van Leeuwen, E. J. D. Vredenbregt, and S. J. J. M. F. Kokkelmans, J. Phys. B **44**, 184008 (2011).
[17] P. Schauß, M. Cheneau, M. Endres, T. Fukuhara, S. Hild, A. Omran, T. Pohl, C. Gross, S. Kuhr, and I. Bloch, Nature **491**, 87 (2012).
[18] P. Schauß, J. Zeiher, T. Fukuhara, S. Hild, M. Cheneau, T. Macrì, T. Pohl, I. Bloch, and C. Gross, arXiv:1404.0980.
[19] A. Schwarzkopf, D. A. Anderson, N. Thaicharoen, and G. Raithel, Phys. Rev. A **88**, 061406 (2013).
[20] C. Ates, T. Pohl, T. Pattard, and J.M. Rost, Phys. Rev. Lett. **98**, 023002 (2007).
[21] T. Amthor, C. Giese, C. S. Hofmann, and M. Weidemüller, Phys. Rev. Lett. **104**, 013001 (2010).
[22] I. Lesanovsky and J. P. Garrahan, Phys. Rev. A **90**, 011603(R) (2014); M. Marcuzzi, J. Schick, B. Olmos, and I. Lesanovsky, J. Phys. A **47**, 482001 (2014).
[23] M. Gärttner, K. P. Heeg, T. Gasenzer, and J. Evers, Phys. Rev. A **88**, 043410 (2013).
[24] H. Schempp, G. Günter, M. Robert-de-Saint-Vincent, C. S. Hofmann, D. Breyel, A. Komnik, D. W. Schönleber, M. Gärttner, J. Evers, S. Whitlock, and M. Weidemüller, Phys. Rev. Lett. **112**, 013002 (2014).
[25] N. Malossi, M.M. Valado, S. Scotto, P. Huillery, P. Pillet, D. Ciampini, E. Arimondo, and O. Morsch, Phys. Rev. Lett. **113**, 023006 (2014).
[26] J. M. Raimond, G. Vitrant, and S. Haroche, J. Phys. B **14**, L655 (1981).
[27] T. Baluktsian, B. Huber, R. Löw, and T. Pfau, Phys. Rev. Lett. **110**, 123001 (2013).
[28] C. Carr, R. Ritter, C. G. Wade, C. S. Adams, and K. J. Weatherill, Phys. Rev. Lett. **111**, 113901 (2013).
[29] R. Heidemann, U. Raitzsch, V. Bendkowsky, B. Butscher, R. Löw, L. Santos, and T. Pfau, Phys. Rev. Lett. **99**, 163601 (2007).
[30] See Supplemental Material at [URL], which includes Refs. [36, 37], for details on the experimental procedure, the adiabatic elimination, the theoretical model, the pair-state potentials, the dephasing mechanism and the size of the aggregates..
[31] B. Huber, T. Baluktsian, M. Schlagmüller, A. Kölle, H. Kübler, R. Löw, and T. Pfau, Phys. Rev. Lett. **107**, 243001 (2011).
[32] K. Singer, J. Stanojevic, M. Weidemüller, and R. Côté, J. Phys. B **38**, S295 (2005).
[33] A. Schwettmann, J. Crawford, K.R. Overstreet, and J.P. Shaffer, Phys. Rev. A **74**, 020701 (2006).
[34] G. Vitrant, J. M. Raimond, M. Gross, and S. Haroche, J. Phys. B **15**, L49 (1982).
[35] The Stark-shift of an ion on the 32S state is C_4/r^4 with $C_4 = 2\pi \times -213$ MHz$\cdot\mu$m^4, which is an attractive potential with comparable strength to the Rydberg-Rydberg potentials. Therefore facilitation would similarly occur around an ion, if created.
[36] A. Urvoy, C. Carr, R. Ritter, C. S. Adams, K. J. Weatherill, and R. Löw, J. Phys. B **46**, 245001 (2013).
[37] P. Siddons, C. S. Adams, C. Ge, and I. G. Hughes, J. Phys. B **41**, 155004 (2008)
.